Biuletyn WAT
Vol. LXVII, Nr 4, 2018

# Identification of numerical model parameters of tunnel lining in non-cohesive soil

PAWEŁ SZKLENNIK

Military University of Technology, Faculty of Civil Engineering and Geodesy,
2. Gen. W. Urbanowicza Str, 00-908 Warsaw, Poland, pawel.szklennik@wat.edu.pl

**Abstract.** The paper discusses identification of numeric model parameters of tunnel lining in a soil medium according to the discrete element method. An author's program based on the discrete element method was used. Laboratory tests were conducted to determine the computer model parameters defining the lining and the soil medium. The numerical model was calibrated by comparing the lining deformations occurring in the laboratory test and in the numeric simulation. Tunnel lining displacement during laboratory tests was determined using digital photography.
**Keywords:** civil engineering, discrete element method, cylindrical tunnel lining
**DOI:** 10.5604/01.3001.0012.8484

## 1. Introduction

Modelling the behaviour of a physical soil medium must reflect its internal structure and mechanisms emerging during deformation. In many cases, it is useful to employ approximations treating the soil medium as a continuous medium with assigned mathematical expressions of physical theories of varied degrees of non-linearity. In these theories, the deformation mechanism is not expressed explicitly. The mechanism is hidden in mathematical differential expressions of geometry and displacement relations, and in equilibrium equations. Even when using numerical analysis methods in accordance with FEM, or finite difference methods, medium discretisation does not change the essence of the basic principle of medium continuity, although it does reduce this principle to a degree. It is believed that the continuous medium model can be considered as consistent with cohesive soil media with a compact structure, which means no marked content of the liquid phase.

For non-cohesive soils, which have a granular structure, analysis results obtained under the continuous model must be interpreted with a degree of caution. This type of medium model ignores the actual deformation mechanisms, which are characterised not by grain deformation but by their mutual displacement. The granular structure of the medium — its framework — changes. The primary interaction within the medium are friction forces, not deformations of grains taking axial forces from adjacent grains. Today it is believed that the proper method of analysing the deformations of such media is defining the medium as granular, while the analysis method is the discrete element method (DEM).

This paper presents the process of identifying the parameters of a DEM numerical model of a non-cohesive soil medium with a flexible model cylinder tunnel lining placed within. Such a model can be used for further numerical analysis of tunnel construction interactions with the surrounding soil medium. This will enable taking into account such factors as the structural flexibility of the lining or imperfections of contact with the soil medium in the analysis.

## 2. Discrete element method

An intrinsic property of non-cohesive soil media is their granular structure, which creates a natural spatial discretisation, usually irregular. Thanks to discrete models, it is possible to take into account the arrangement of individual particles, their mutual overlap, changes in the medium's density as a result of loading and unloading, and the effects of the medium's grain size distribution on test results. One major method of this kind is the Discrete Element Method (DEM) [4]. This method is chiefly used to analyse dynamics problems [3, 15]. Its sample applications in loose medium studies include simulations of direct shear [12, 17] and triaxial compression [14].

It can be employed to model, among others, the behaviour of naturally fissured rock that undergoes further fragmentation, for example as a result of tunnel boring without installing any linings [2], or the behaviour of concrete — papers [6, 7]. The drawbacks of discrete methods include fairly high processing load during simulations of complex problems, caused by the very high number of elements. This entails a long duration of simulations. It is one of the reasons why it is proposed to combine continuous and discrete modelling, e.g. FEM and DEM, in a single simulation [5], [10], [11]. Furthermore, DEM has successfully been used to analyse, for example, the behaviour of solid rock [13].

### 2.1. Theoretical basics of DEM

The idea of the method in question is modelling a loose medium directly as a set of individual particles with a specific shape, which can interact with one another

with contact forces calculated in accordance with the assumed local contact model. Due to significant simplifications during numerical searching for contacting elements, the frequently used shapes include spheres (3D), cylinders (2D) and elements formed of interpenetrating or "patched together" spheres or cylinders. Elliptical elements are also used on occasion [16]. The basic operations performed during the computations are: searching for pairs of elements in contact, calculating contact interactions between them, updating element positions based on motion equations. The model of the material is described using constitutive relations for local contact between individual elements. Depending on the material described, the contact may take the form of a permanent tension-resistant bond, or a non-permanent bond. A permanent bond can be broken if the affecting force has a sufficient value. For loose materials, contact is non-permanent. This type of contact can also occur in the event that particles modelling a solid material, whose bond was previously severed, come into contact again. Generally, the constitutive contact model takes into account inter-element interactions in the form of forces and possibly moments, resulting from a certain assumed rigidity of bonds, friction and damping. A fairly simple example is the perfect brittle-elastic model. More complex instances include models with gradually decreasing bond rigidity and elastic-plastic models with softening effect.

## 2.2. Calculating contact interactions

Contact forces are calculated using a constitutive model of contact between two elements, shown in Fig. 1. Generally, such contact can be treated as "soft" [4] or "rigid". For rigid contact, only post-impact velocities of elements are calculated, the forces of interactions between them are not determined. Under "soft" contact, a minor interpenetration of discrete elements is allowed on impact, which can be treated as micro-scale deformation of the given particles. In this study the "soft" contact model is used. It is described with a rigidity modulus for the axial ($k_n$) and contact direction ($k_s$), a damping factor $c_n$ and a sliding friction factor μ. The software utilised also enables taking into account rolling friction and external damping, which are described further in this paper.

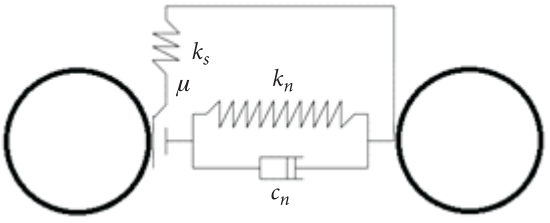


Fig. 1. Model of contact between two discrete elements

The contact force at the point of contact between elements can be decomposed into the tangent $F_s$ and normal $F_n$ constituents (Fig. 2). The normal contact force $F_n$ can in turn be decomposed into the elastic $F_n^s$ and damping $F_n^t$ constituents.

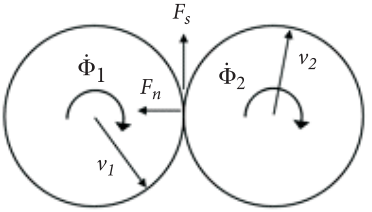


Fig. 2. Element interactions and the contact model

### *2.2.1. Normal contact force*

Decomposing the normal force into the elastic and damping constituents yields the following formula

$$F_n = F_n^s + F_n^t. \tag{1}$$

The elastic constituent is calculated as

$$F_n^s = k_n \cdot g_n, \tag{2}$$

where $g_n$ means mutual "overlapping" of elements (Fig. 3) at the given moment, calculated as $g_n = l_c - r_i - r_j$.

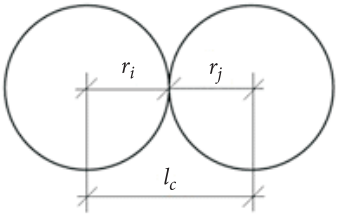


Fig. 3. Elements in contact (case $g_n = 0$)

The damping constituent, on the other hand, is calculated for viscous damping according to the following formula

$$F_n^t = c_n \cdot v_{nw}, \tag{3}$$

where $v_{nw}$ is the normal constituent of relative velocity at the point of contact between elements. It is convenient to relate the damping to the critical damping value $c_{cr}$ using the factor $\alpha_c$ and the following relation

$$c_n = \alpha_c \cdot c_{cr}. \tag{4}$$

On contact between two discrete elements connected with a spring of rigidity $k_n$, the critical damping value is

$$c_{cr} = 2\sqrt{\left(m_1 m_2 k_n\right)/\left(m_1 + m_2\right)}, \tag{5}$$

where $m_1$ and $m_2$ are the element masses.

### *2.2.2. Tangent contact force*

If there is no cohesion, the tangent force is calculated according to the so-called regularised Coulomb friction model, shown in Fig. 4. The maximum possible value of the friction force is therefore

$$F_s^{\max} = \mu\left|F_n\right|. \tag{6}$$

The tangent force value in the given local contact is updated based on the values of the so-called incremental slide $\mathbf{u}_{sw}$ and of tangent rigidity, according to the following formula

$$\mathbf{F}_s^{prob} = \mathbf{F}_s^{n-1} + k_s \cdot \Delta\mathbf{u}_{sw}, \tag{7}$$

where $\mathbf{F}_s^{prob}$ is the so-called trial value of tangent force.

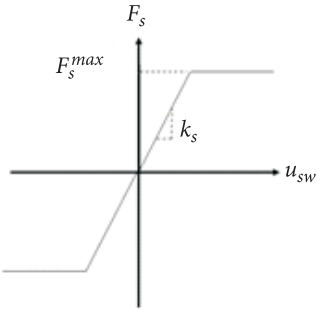


Fig. 4. Regularised Coulomb friction model used in DEM [10].

Next, if $\left\|\mathbf{F}_s^{prob}\right\| \le F_s^{\max}$, then the new (current) friction force

$$\mathbf{F}_s^{akt} = \mathbf{F}_s^{prob}, \tag{8}$$

while if $\left\|\mathbf{F}_s^{prob}\right\| \le F_s^{\max}$, then

$$\mathbf{F}_s^{akt} = F_s^{\max} \cdot \frac{\mathbf{F}_s^{prob}}{\left\|\mathbf{F}_s^{prob}\right\|}. \tag{9}$$

The value of the so-called incremental slide is defined by

$$\Delta \mathbf{u}_{sw} = \mathbf{v}_{sw} \cdot \Delta t, \tag{10}$$

where $\mathbf{v}_{sw}$ is the vector of the tangent relative linear velocity constituent $\mathbf{v}_w$ at the point of contact calculated based on linear $\mathbf{v}$ and angular $\dot{\Phi}$ velocities of the colliding elements (Fig. 2). Relative linear velocity at the point of contact is calculated as

$$\mathbf{v}_w = \left(\mathbf{v}_\mathbf{j} + \dot{\Phi}_\mathbf{j} \times \mathbf{r}_\mathbf{j}\right) - \left(\mathbf{v}_\mathbf{i} + \dot{\Phi}_\mathbf{i} \times \mathbf{r}_\mathbf{i}\right), \tag{11}$$

and then

$$\mathbf{v}_{sw} = \mathbf{v}_w - \left(\mathbf{v}_\mathbf{w} \cdot \mathbf{n}_\mathbf{i}\right)\mathbf{n}_\mathbf{i}, \tag{12}$$

where $\mathbf{n}_\mathbf{i}$ is the unit vector normal to the plane of contact.

### *2.2.3. Rolling friction resistance*

This resistance $\mathbf{M}_f$ is determined based on relative rotational speed at the point of contact $\dot{\Phi}_w$, the assumed "rolling resistance rigidity" $k_\theta$ and the rolling friction factor $f$, in the same manner as sliding friction resistance. The $f$ value can be calculated as part of a discrete element radius ($r_k$) using the ε factor according to formula $f = \varepsilon \cdot r_k$. The maximum possible rolling resistance value is therefore

$$M_f^{\max} = f \cdot \left|F_\mathrm{n}\right|. \tag{13}$$

In the three-dimensional model, the resistance acting around the axis perpendicular to the plane of contact between spheres and acting around the axis lying in this plane is calculated separately. Analyses of the effects of rolling resistance in DEM can be found in papers [8, 9], while a comparative analysis of different rolling resistance models, including methods of calculating $k_\theta$, are presented in paper [1]. The use of the right values of the sliding and rolling friction parameters is important, particularly for simulations where the effects of roughness and irregularity of the surface of elements of the given medium must be represented.

Other than the interactions already discussed, initial stresses in the medium are also important for soils, and they can be taken into account at the start of the computations as an initial state condition.

## 2.3. Motion equations of elements

For the purposes of performing the numerical simulations, the simulation time assumed at the start of the computations is divided into time steps Δt. At each time

step, linear and rotational accelerations are calculated according to Newton's motion equations for each cylindrical (2D) or spherical (3D) element. The matrix notation for a single element in linear motion is

$$\mathbf{m}_i \cdot \ddot{\mathbf{U}}_i = \mathbf{F}_i^{calk}, \tag{14}$$

where $\mathbf{m}_i$ is the matrix of masses of the $i$ discrete element, $\ddot{\mathbf{U}}_i$ is the linear acceleration vector, and $\mathbf{F}_i^{calk}$ is the vector of the resultant forces acting on the element.

For rotational motion, the formula is

$$\mathbf{J}_i \cdot \ddot{\Phi}_i + \dot{\Phi}_i \times \mathbf{J}_i \cdot \dot{\Phi}_i = \mathbf{M}_i^{calk}, \tag{15}$$

where $\mathbf{J}_i$ is the matrix of inertia moments for the discrete element, $\ddot{\mathbf{\Phi}}_i$ is the vector of rotational accelerations, $\dot{\mathbf{\Phi}}_i$ is the angular velocity vector, while $\mathbf{M}_i^{calk}$ is the external moments vector.

In order to determine the velocities and displacements, motion equations are integrated using the explicit or implicit method. Due to the significantly lower computation cost — no need to solve a system of equations — the explicit method is frequently used.

This requires limiting the time step value Δt to the critical value equal

$$\Delta t_c = \left(2/\omega_{\max}\right)\left(\sqrt{1+\eta^2} - \eta\right), \tag{16}$$

where $\omega_{\max}$ is the highest natural frequency of the system, while $\eta$ defines the ratio of the damping used to critical damping for free vibrations with a frequency of $\omega_{\max}$.

## 3. Author's DEM software

The author's software uses the "soft" contact model described earlier in this paper. This model, discussed in paper [4], assumes a linear relation between element rigidity and its size. Elastic contact between two particles is analysed as for two elements with a specific rigidity, arranged in series. The rigidities of elements 1 and 2 in contact are therefore

$$k_{n,1} = \frac{E_1 A_1}{d_1}, \tag{17}$$

$$k_{n,2} = \frac{E_2 A_2}{d_2}, \tag{18}$$

where $E_1$ and $E_2$ are element elasticity moduli, $d_1$ and $d_2$ are the assumed lengths of hypothetical elastic elements corresponding to the discrete elements, while $A_1$

and $A_2$ are the surface areas of "cross-sections" of the elastic elements. Ultimately, the local rigidity of contact of two given discrete elements is

$$k_n = \frac{k_{n,1} \cdot k_{n,2}}{k_{n,1} + k_{n,2}}. \tag{19}$$

In order to determine sliding and rolling friction resistance, an approach discussed, for example in [14], was used. Rigidity at the tangent direction was assumed as $k_s = k_n \nu^c$, where $\nu^c$ is the so-called Poisson's ratio for local contact. Rolling resistance rigidity $k_\theta = \beta k_s r_1 r_2$, where $\beta$ is a certain proportionality ratio, while $r_1$ and $r_2$ are radii of the elements in contact. Rolling friction factor $f = \varepsilon \cdot r_{sr}$, where $r_{sr}$ is the average length of the radius of two elements in contact.

The values of all parameters listed in this and the previous section need to be defined appropriately for the type of granular medium, its fractions, shape of elements and the properties of their surface.

In the software used in this study the contact interactions included the axial and tangent force. As internal friction in a gravel medium is the result of the combined effects of sliding friction and rolling resistance between particles, rolling friction is also taken into account in the contact between elements of the soil medium. A summary of the model's parameters related to material characteristics and element contact, together with their respective symbols, is shown in Tables 1 and 2. The indexed symbols mean the given material or pairs of surfaces in contact.

Table 1

Material parameters of the numerical model

| Material parameter | Material | |
|---|---|---|
| | soil medium (gravel) | lining (HDPE) |
| Young's modulus | $E_z$ | $E_{ob}$ |
| Particle density | $\rho_z$ | $\rho_{ob}$ |

Table 2

Contact parameters of the numerical model

| Contact parameter | Contact type | | | |
|---|---|---|---|---|
| | gravel – gravel | lining – lining | lining – gravel | edge – gravel |
| Poisson's ratio | $\nu_z^c$ | $\nu_{ob}^c$ | $\nu_{ob-z}^c$ | $\nu_{b-z}^c = \nu_z^c$ |
| proportionality ratio for defining rolling resistance rigidity | $\beta_z$ | absent | $\beta_{ob-z}$ | $\beta_{b-z}$ |
| sliding friction factor | $\mu_z$ | absent | $\mu_{ob-z}$ | $\mu_{b-z}$ |
| parameter for defining the rolling resistance factor | $\varepsilon_z$ | absent | $\varepsilon_{ob-z}$ | $\varepsilon_{b-z}$ |
| viscous damping factor | $\alpha_{c,z}$ | absent | $\alpha_{c,ob-z}$ | $\alpha_{c,b-z}$ |

## 4. Laboratory tests

As has been mentioned earlier, the correctness of DEM analysis results depends on the assumed model parameters. In the case in question, it will be these elements in particular that characterise the internal resistance of a granular medium. Therefore they need to be determined, for example using experimental tests. In this study, a non-densified gravel granular medium was considered. Parameter models were sought for in an indirect manner. This involved placing a flexible cylindrical tunnel lining in the soil medium. The growing quasi-static load applied caused changes in the structure of the soil. These changes caused deformations of the lining, which were recorded. The problem of theoretical calculation of these deformations was solved using author's DEM software, where various sets of the given internal parameters were used. A set was sought that would represent the lining's deformations with the smallest error.

Laboratory tests were conducted using a box with transparent polycarbonate walls — Fig. 5. The test space dimensions of the box were 0.90 × 0.58 m. The external walls were strengthened with metal clamping plates on both sides and local lateral braces. The side walls were covered with a friction reducing agent on the inside.

Fig. 5. View of the test station

As the soil medium, gravel with $\Phi_{el}$ = 2 ÷ 4 mm grains was used. Bulk density of the non-densified soil was calculated as $\rho_{o,z} = 1524 \ \frac{\text{kg}}{\text{m}^3}$, the particle density

of the soil was $\rho_{s,z} = 2550 \frac{\text{kg}}{\text{m}^3}$. The value of the internal friction angle for loose gravel, determined in a direct shear test, was $\varphi_z$ = 37,6°. On this basis, the active pressure factor of $K_a$ = 0,24 was calculated.

A flexible cylindrical lining made of high-density polyethylene (HDPE), with a diameter of 90 mm and wall thickness of 0.75 mm was placed in the soil medium. The length of the lining corresponded to the internal length of the box, which was $L_{ob}$ = 143 mm. Based on the tension test, the mean Young's modulus value for HDPE $E_{ob}$ = 500 MPa was calculated. Material density was determined as $\rho_{ob} = 1100 \frac{\text{kg}}{\text{m}^3}$.

Gravel was poured on the lining in the box up to the assumed layer height, in this case equal to the lining's diameter, i.e. 90 mm. The external load, applied in the surcharge surface symmetrically to the vertical axis of the lining, was a bag filled with a gradually increased amount of gravel. This enabled a more uniform distribution of the external load. The resultant force of the constant load grew during the test from 0 to 1250 N. The width of the field under load was 450 mm. Twelve markers were attached to the perimeter of the lining, which served as measurement points during displacement analysis. The test model during loading and the lining marker arrangement are shown in Figure 6.

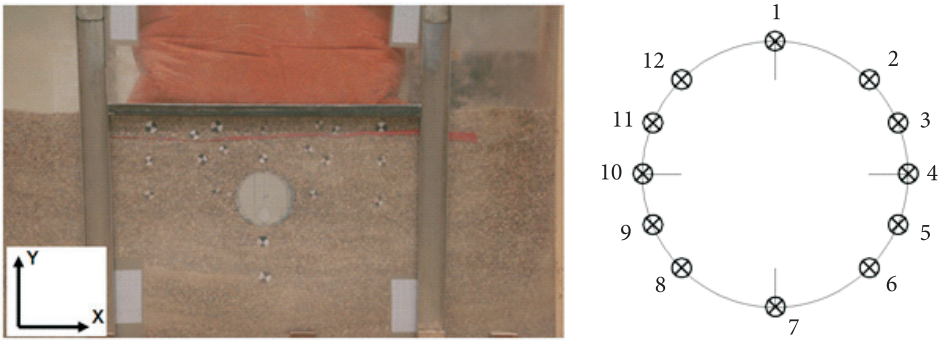


Fig. 6. Test station during loading and marker arrangement on the perimeter of the flexible cylindrical lining

Markers were also placed inside — this can be seen in Fig. 6. However, direct recording of framework deformation changes did not prove to be useful for drawing conclusions on the values of internal soil resistance parameters. Tunnel lining deformation was measured by digital photography using a Canon EOS 400D Digital camera. Before the tests were commenced, pixel size was determined — the number of pixels in an image corresponding to a unit of actual length. Next, images were taken at equal time intervals during the entire lining deformation process. *X* and *Y* coordinates for each marker, determined before and after the tests and specified

in pixels in the images, were used to determine the actual changes in positions of these points in space. Laboratory test results were calculated as averages of the two tests conducted. They are presented in section 6, together with a comparison to the displacement values obtained numerically using the discrete element method.

## 5. Numerical model of tunnel lining interaction with the loaded soil medium

The author's software was used to model the system built in the laboratory tests. The soil was modelled using cylindrical elements — such a description can be considered as representing a flat state of stress (2D). Attempts at analyses using a 3D model led to very long computation times without a marked qualitative change in the results, and for this reason the model was abandoned.

The numerical simulations were conducted on a medium containing 43,756 cylinders corresponding to the analysed gravel medium. A list of parameters used to numerically define the medium and lining has already been provided in Tables 1 and 2. A sample numerical model is graphically shown in Figs. 7 and 8. The width of the soil medium along the X axis was 80 cm. Because the system was reduced to a two-dimensional form, the maximum diameter of the discrete elements was reduced compared to the corresponding maximum gravel grain diameter in the laboratory tests. Thus the dimensions of the cylindrical elements were $\Phi_{el}^{DEM} = 2 \div 2.5$ mm. The maximum (end) value of the resultant force of surcharge load Q was 1250 N. As in the laboratory test, it was applied as an evenly distributed load, symmetrically to the vertical axis of the tunnel lining. The time step defined based on its critical value and on observations of stability and convergence of numerical solutions was set as $\Delta t = 5.5 \cdot 10^{-7}$s. The total number of time steps, encompassing the time of load increase and system stabilisation, was 4,500,000. Based on an analysis of particle behaviour during the end period of the simulation, it was determined that the model can generally be treated as quasi-static.

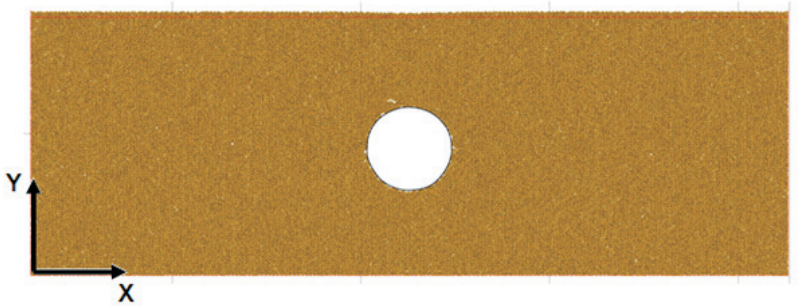


Fig. 7. Discrete DEM model

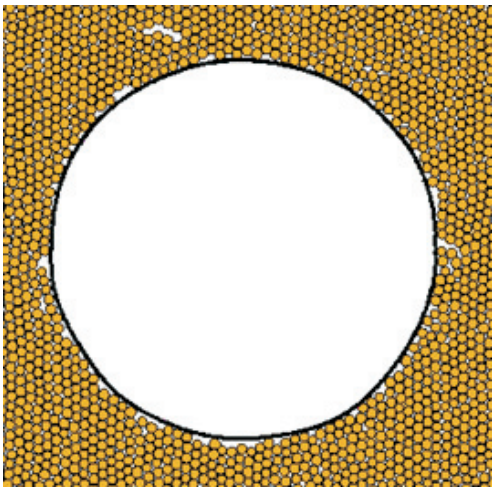

Fig. 8. A close-up on the tunnel lining

The cylindrical lining with a 0.75 mm thickness was modelled as a ring with a wall composed of 5,239 cylindrical elements with a 0.2 mm diameter. In this manner, the actual thickness could approximately be achieved. In the computer program it was assumed that the lining construction reacted in a perfectly elastic manner. Fig. 8 shows an illustration of the possible imperfections affecting resistance in the contact area of the numerically modelled gravel medium with a cylindrical lining. They are generated intrinsically during the preparation process of the initial state of the medium for the purposes of numerical analysis. They can therefore be treated as deviations from the perfect state — a certain dose of realism in the numerical model, bringing it closer to reality.

## 6. Calibration of the numerical model

Performing a simulation of the behaviour of a discrete medium requires defining the values of the parameters characterising its numerical model. These parameters were preliminarily divided — considering their impact — into two groups, primary and secondary. The most important factors were considered those that decided the rigidity of the soil structure and the tunnel lining, as well as certain imperfections in the structure of the soil. Therefore, primary parameters included those that describe contact between elements of the soil medium and mutual contact of the lining's elements. Secondary parameters included all other values, e.g. the damping and rigidity factors that should enable achieving specific medium resistance values while maintaining stability of the computation.

Poisson's ratio for mutual contact of lining elements was defined as equal to Poisson's ratio for HDPE $\nu_{ob}^{c} = 0.45$. The elasticity modulus of the soil elements was defined as $E_z = 9$ MPa,, and Poisson's ratio as $\nu_z^c = 0.15$, which ensured its sufficient rigidity and enabled achieving the required friction resistances. In all preliminary analysis simulations of secondary parameters, the same sliding $\mu_z = 0.3$ and rolling friction $\varepsilon_z = 0.3$ parameters were assumed, as these are primary parameters. After verification, due to the minimal impact, the proportionality parameters for determining the rolling friction of edge-gravel and lining-gravel contact were classified as secondary parameters. These were set as $\beta_{b-z} = 0.04$ and $\beta_{ob-z} = 0.04$. The parameter determining the rolling resistance of edge-gravel contact was set as $\varepsilon_{b-z} = 0.3$. For any type of cohesionless contact, the parameter for determining viscous damping was set as $\alpha_c = 0.5$. No external damping was introduced in the description of soil medium element motion.

During preliminary analyses, the effects of changing individual parameters on the behaviour of the numerical model were investigated — any differences in deformations of the lining or its surrounding medium were compared. Due to the significant number of results, only end conclusions drawn on their basis are presented here. Specifically, no major effect of increasing the weight of the lining to the value of $\rho_{ob} = 10000 \ \frac{\text{kg}}{\text{m}^3}$ were observed. This increase was done due to the increased critical step value, and consequently the ability to use much longer time steps in the numerical procedure. This saved a significant amount of time on the duration of the numerical analyses.

No major effect of changes in Poisson's ratio values in the lining's contact with the soil were observed, and consequently no variants of it were used. Because the box walls in the laboratory test were covered with a friction preventing agent, the coefficients of sliding friction between the soil medium and edge were limited to the value of 0.3. A similar limit value was set for sliding friction in contact between the lining and the soil medium — it is a contact modelling the interface between polyethylene and the gravel. In both cases, as well as for the rolling friction factor for the contact between lining and soil medium elements, no major effects of said parameters on lining deformation and the behaviour of its surrounding soil medium were observed. During the last phase of the preliminary tests, mainly the stability of the numerical process at the given value of the proportionality factor $\beta_z$ used to determine the rolling resistance rigidity was verified, up to values resulting in loss of said stability. Ultimately, $\beta_z = 50$ was adopted as the value that enabled achieving the right rolling resistances without loss of computation stability. Also in the other contact types, $\beta_{b-z} = 50$ and $\beta_{ob-z} = 50$ were ultimately set. The final parameters defined after preliminary analyses are summarised in Table 3.

Table 3

Contact parameters defined after the preliminary analysis series

| Contact parameter | Contact type | | | |
|---|---|---|---|---|
| | gravel – gravel | lining – lining | lining – gravel | edge – gravel |
| Poisson's ratio | $\nu_z^c = 0.15$ | $\nu_{ob}^c = 0.45$ | $\nu_{ob-z}^c = 0.3$ | $\nu_{b-z}^c = 0.15$ |
| proportionality ratio for defining rolling resistance rigidity | $\beta_z = 50$ | absent | $\beta_{ob-z} = 50$ | $\beta_{b-z} = 50$ |
| sliding friction factor | analysed during the main phase | absent | $\mu_{ob-z} = 0.1$ | $\mu_{b-z} = 0.1$ |
| parameter for defining the rolling resistance factor | analysed during the main phase | absent | $\varepsilon_{ob-z} = 0.1$ | $\varepsilon_{b-z} = 0.1$ |
| viscous damping factor | $\alpha_{c,z} = 0.5$ | absent | $\alpha_{c,ob-z} = 0.5$ | $\alpha_{c,b-z} = 0.5$ |

During the final identification stage, simulations were performed where the variables were only the parameters of sliding friction $\mu_z$ and rolling friction $\varepsilon_z$ between elements modelling the soil medium. These are two most important parameters that decide the magnitude of deformation of the medium and its load-bearing capacity under the contact rigidity parameters defined earlier. The values of these parameters were sought for within the $\mu_z = (0.1 \div 0.7)$ and $\varepsilon_z = (0.1 \div 0.7)$ ranges.

Among all the analyses performed, those were selected where tunnel lining destruction — i.e. loss of stability — did not occur. In order to finally define the model closest to reality, displacements of measurement points arranged along the lining's perimeter (Fig. 6) in DEM simulations (Δ DEM) were compared with corresponding displacements of markers in the laboratory tests (Δ LAB). Based on the differences in their values, the total relative error was calculated for each case using the following formula

$$\sum \vartheta_W = \sum_{i=1}^{24} \frac{\left|\Delta_{DEM,i} - \Delta_{LAB,i}\right|}{\left|\Delta_{LAB,i}\right|}, \tag{20}$$

and total squared error using

$$\sum \vartheta_K = \sum_{i=1}^{24} \left[ \left(\Delta_{DEM,i} - \Delta_{LAB,i}\right)^2 \right]. \tag{21}$$

Several such cases and their $\mu_z$ and $\varepsilon_z$ values are shown in Table 4. The error values calculated for these cases using formulas 20 and 21 are shown in Table 5.

Table 4

Friction parameter combinations not causing lining destruction, determined after the main simulation phase

| Simulation No. | Model parameter | |
|---|---|---|
| | $\mu_z$ | $\varepsilon_z$ |
| 1 | 0.50 | 0.10 |
| 2 | 0.70 | 0.10 |
| 3 | 0.25 | 0.40 |
| 4 | 0.30 | 0.40 |

Table 5

Error values in DEM simulations compared to laboratory results

| | $\sum \vartheta_K$ | $\sum \vartheta_W$ |
|---|---|---|
| Δ DEM (1) | 5.37 | 13.19 |
| Δ DEM (2) | 5.57 | 11.71 |
| Δ DEM (3) | 3.08 | 11.44 |
| Δ DEM (4) | 4.09 | 13.36 |

These values indicate that the lowest relative and squared error occurred in DEM simulation no. 3. The parameter set used in this simulation was accepted as characterising the soil medium that is the closest representation of the behaviour of the system used in the laboratory tests.

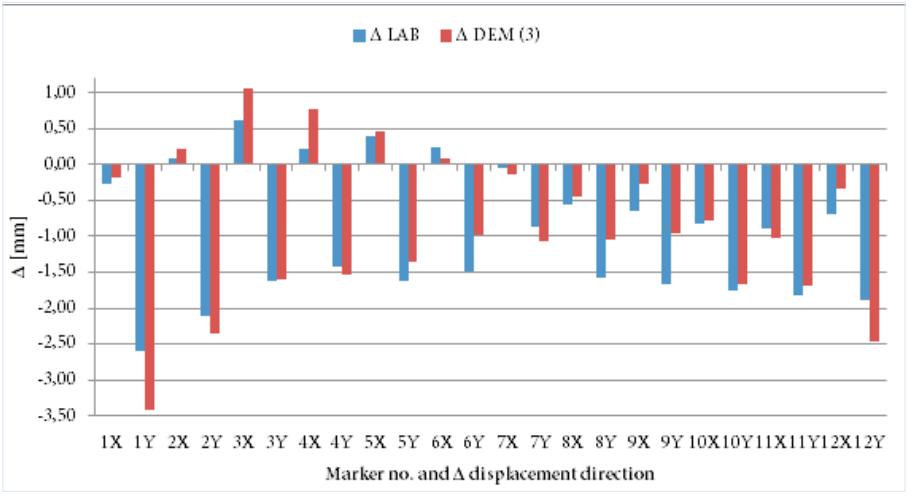


Fig. 9. Distribution of tunnel lining points displacement values according to DEM simulation (3) and obtained from laboratory tests

Figure 9 shows a graphical illustration of the distribution of tunnel lining displacement values obtained in the laboratory test, compared to corresponding displacements from the DEM simulation with the lowest error (no. 3). The consistent signs of displacements in all cases of vertical and horizontal displacement is notable, as it indicates a good description of the form of tunnel lining deformation in the numerical simulation.

## 7. Summary

The study proved that tunnel lining behaviour in non-cohesive soil was modelled correctly using the numerical discrete element method. In order to perform the numerical analyses, it was necessary to build a model of the whole system subjected to the laboratory test, so that the actual conditions and reactions of the test medium and its model structure could be represented as closely as possible. The process of identifying the parameters of such numerical models was demonstrated, which involved comparing the deformations of the actual tunnel lining loaded in the laboratory test with the virtual model. Some material parameters of the numerical model that have physical equivalents were defined based on direct tests of the lining material and soil, while the others were defined indirectly through tests, selecting the model with the deformations closest to real values.

The analysis demonstrated that the most important soil parameters, which decided the soil structure load-bearing capacity and tunnel lining deformations, were sliding and rolling friction factors in this case. The final numerical model enables taking into account the interactions between soil and lining during the loading process, and also enables representing the imperfections of contact between soil grains, which can evolve during structure deformation. These abilities are gained precisely due to using discrete methods, which for such models have a specific advantage over continuous modelling.

The study has been carried out within the framework of the statutory research no. 934, carried out in the Faculty of Civil Engineering and Geodesy of the Military University of Technology.

*Received June 18, 2018. Revised October 3, 2018.*

Paper translated into English and verified by SKRIVANEK sp. z o.o., 22 Solec Street, 00-410 Warsaw, Poland.

REFERENCES

[1] Ai J., Chen J., Rotter J. M., Ooi J. Y., *Assessment of rolling resistance models in discrete element simulations*, Powder Technology, 206, 30, 2011, 269–282.

[2] Boon C., *Distinct Element Modelling of Jointed Rock Masses: Algorithms and Their Verification*, PhD thesis, St Cross College, Oxford, 2013.

[3] Bourrier F., Nicot F., Darve F., *Evolution of the micromechanical properties of impacted granular materials*, Comptes Rendus Mecanique, 338, 10–11, 2010, 639–647.

[4] Cundall P. A., Strack O. D. L., *A discrete numerical model for granular assemblies*. Géotechnique, 29, 1, 1979, 47–65.

[5] Han K., Peric D., Crook A. J. L., Owen D. R. J., *A combined finite/discrete element simulation of shot peening processes – Part I: studies on 2D interaction laws*, Eng. Comput., 17, 5, 2000, 93–620.

[6] Hentz S., Daudeville L., Donzé F. V., *Identification and validation of a discrete element model for concrete*, ASCE J. Eng. Mech., vol. 130, 2004, 709–719.

[7] Hentz S., Donzé F. V., Daudeville L., *Discrete element modelling of concrete submitted to dynamic loading at high strain rates*, Computers and Structures, vol. 82, 2004, 2509–2524.

[8] Iwashita K., Oda M., *Rolling Resistance at Contacts in Simulation of Shear Band Development by DEM*, Journal of Engineering Mechanics, 124, 3, 1998, 285–292.

[9] Jiang M. J., Yu H.–S., Harris D., *A novel discrete model for granular material incorporating rolling resistance*, Computers and Geotechnics, 32, 5, 2005, 340–357.

[10] Oñate E., Rojek J., *Combination of discrete element and finite element methods for dynamic analysis of geomechanics problems*, Computer Methods in Applied Mechanics and Engineering, 2004, 3087-3128.

[11] Rojek J., *Modelowanie i symulacja komputerowa złożonych zagadnień mechaniki nieliniowej metodami elementów skończonych i dyskretnych*, IPPT PAN, Warszawa, 2007.

[12] Szklennik P., *Numeryczne analizy bezpośredniego ścinania gruntu niespoistego z zastosowaniem metody elementów dyskretnych*, Budownictwo i Inżynieria Środowiska, 3, 4, 2012, 211–216.

[13] Wang Y., Tonon F., *Calibration of a discrete element model for intact rock up to its peak strength*, Int. J. Numer. Anal. Meth. Geomech., vol. 34, 2010, 447–469.

[14] Widuliński Ł., Kozicki J., Tejchman J., *Numerical Simulations of Triaxial Test with Sand Using DEM*, Archives of Hydro-Engineering and Environmental Mechanics, 56, 3–4, 2009, 149–172.

[15] Wu L., Guan T., *Discrete element model for analysis of chamber pressure of earth pressure balance shield machine*, Proceedings of 2010 International Conference on Mechanic Automation and Control Engineering (MACE), 2010, 671–674.

[16] Yan B., Regueiro R. A., Sture S., *Three-dimensional ellipsoidal discrete element modeling of granular materials and its coupling with finite element facets*, Engineering Computations: International Journal for Computer Aided Engineering and Software, 27, 4, 2010, 519-550.

[17] Yan Y., Ji S., *Discrete element modeling of direct shear tests for a granular material*, International Journal for Numerical and Analytical Methods in Geomechanics, 34, 9, 2010, 978–990.

P. SZKLENNIK

## Identyfikacja parametrów modelu numerycznego obudowy tunelowej w gruncie niespoistym

**Streszczenie.** W pracy przedstawiono identyfikację parametrów modelu numerycznego modelowej obudowy tunelowej w ośrodku gruntowym według metody elementów dyskretnych. Wykorzystano autorski program oparty na metodzie elementów dyskretnych. W celu określenia parametrów modelu komputerowego charakteryzujących obudowę i ośrodek gruntowy przeprowadzono badania laboratoryjne. Kalibrację modelu numerycznego wykonano przez porównanie deformacji obudowy występującej w badaniu laboratoryjnym i symulacji numerycznej. Przemieszczenia obudowy podczas badań laboratoryjnych wyznaczano za pomocą fotografii cyfrowej.

**Słowa kluczowe:** budownictwo, metoda elementów dyskretnych, obudowa walcowa
**DOI:** 10.5604/01.3001.0012.8484